International Conference on Reactor Physics, Nuclear Power: A Sustainable Resource
Casino-Kursaal Conference Center, Interlaken, Switzerland, September 14-19, 2008

The impact of ^{238}U resonance elastic scattering approximations on thermal reactor Doppler reactivity

Deokjung Lee[a,*], Kord Smith[a], Joel Rhodes[a]

[a] *Studsvik Scandpower Inc., Idaho Falls, USA*

Abstract

The effects of accurate modeling of neutron scattering in ^{238}U resonances are analyzed for typical light water reactor (LWR) and next generation nuclear plant (NGNP) lattices. An exact scattering kernel is formulated and implemented in a newly developed Monte Carlo code, MCSD (Monte Carlo Slowing Down), which solves a neutron slowing down in an infinite homogeneous medium and is used to generate resonance integral data used in the CASMO-5 lattice physics code. It is shown that the exact scattering kernel increases LWR Doppler coefficients by ~10% relative to the traditional assumption of asymptotic elastic downscatter for ^{238}U resonances. These resonance modeling improvements are shown to decrease hot full power eigenvalues by ~200 pcm for LWRs and ~450 pcm for NGNPs.

1. Introduction

NJOY (MacFarlane and Muir, 2000) is commonly used to prepare cross section data for use in downstream lattice physics codes (e.g., CASMO, CENTRUM, HELIOS, LANCER, PARAGON, etc.) and numerous multidimensional neutronics codes (e.g., MCNP, KENO, etc.). NJOY Doppler broadens cross sections for user-specified temperatures, and employs an asymptotic scattering model (i.e., assumes that the nucleus is at rest in the laboratory system) for neutron/nucleus elastic scattering interactions in the epithermal energy region.

As a consequence of this assumption, all deterministic neutronics codes employing NJOY generated cross sections implicitly make the assumption that elastic scattering events in the epithermal range can be well approximated by the asymptotic slowing down model and upscattering events are ignored. Some Monte Carlo codes approximate the elastic scattering probability density function (pdf) as (X-5 Monte Carlo Team, 2003):

$$p(\mu,V)=\frac{\sigma_s(v_r)v_r M(V)}{2\sigma_s^{eff}(v_n)v_n}, \qquad (1)$$

where $\sigma_s(v)$ is the scattering cross section at 0K, $\sigma_s^{eff}(v_n)$ is the Doppler-broadened scattering cross section, v_r is the relative velocity between a neutron with a velocity v_n and a target nucleus moving with a scalar velocity V, μ is the cosine of the angle between the neutron and the target, and $M(V)$ is the pdf for the Maxwellian distribution of target velocities. The pdf is often approximated as:

$$p(\mu,V)\propto v_r M(V), \qquad (2)$$

where Eq. (1) has been simplified by assuming that the variation of $\sigma_s(v_r)$ can be ignored (Carter and Cashwell, 1975). This assumption is quite good for

* Deokjung Lee, deokjung.lee@studsvik.com
Tel: +1 (208) 522-9854, Fax: +1 (208) 522-1187

light isotope scattering, but is far from true for heavy resonance scatterers such as ^{238}U. This assumption is rationalized by noting that heavy nuclides contribute little to neutron moderation because of the large mass difference between neutrons and heavy nuclides.

These assumptions have been previously questioned by numerous researchers (Ouisloumen and Sanchez, 1991; Bouland et al.; Kolesov and Ukraintsev, 2006; Dagan and Broeders, 2006). In fact, Ouisloumen and Sanchez (1991) have shown that heavy nuclide scattering resonances can have a large effect on the average energy of scattered neutrons. They demonstrated that at certain energies near the resonance peaks the average scattered neutron energy actually exceeds the incident neutron energy. Studies have also shown that the asymptotic elastic scattering approximation can lead to a significant underprediction of the Doppler feedback effect in LWRs (Bouland et al.; Kolesov and Ukraintsev, 2006; Dagan and Broeders, 2006).

In this paper, the effects of various resonance scattering models are investigated using an infinite-medium neutron slowing down code, MCSD, which is described here. This code performs a Monte Carlo simulation of neutron slowing down in the resolved resonance energy range and permits elastic scattering to be modeled with either the asymptotic or the exact scattering kernels. MCSD has been used to quantify the impact of the asymptotic scattering approximation. A method for capturing the physics of the exact scattering kernel and generating cross sections for downstream deterministic codes is presented. This method has been incorporated into the resonance treatment of CASMO-5 (Rhodes et al., 2006), which is used to study the effects of the various scattering kernels.

2. Monte Carlo solver for neutron slowing down

2.1. Neutron slowing down problem

The neutron slowing down equation for a homogeneous mixture of three materials in an infinite medium can be formulated, as in NJOY (MacFarlane and Muir, 2000), as:

$$\begin{aligned}\left[\sigma_b + \sigma_t(E)\right]\phi(E) = {} & \frac{(\sigma_b - \sigma_{sm})}{E} \\ & + \int_E^{E/\alpha_m} \sigma_{sm} K_m(E' \to E)\phi(E')dE' \\ & + \int_{E_{\min}}^{E_{\max}} \sigma_{sf}(E') K_f(E' \to E)\phi(E')dE'\end{aligned}, \quad (3)$$

where σ_b is the user-specified energy-independent background cross section, σ_{sm} is the admixed moderator energy-independent scattering cross section, and $\sigma_{sf}(E')$ is the resonance material energy-dependent scattering cross section.

The scattering kernel of the admixed moderator can be expressed by its asymptotic form

$$K_m(E' \to E) = \begin{cases} \dfrac{1}{(1-\alpha_m)E'} & \text{for } \alpha_m E' \le E \le E' \\ 0 & \text{otherwise} \end{cases}, \quad (4)$$

where $\alpha_m = (A-1)^2/(A+1)^2$ and A is the ratio of the masses of the admixed moderator to a neutron. The scattering kernel of the resonance material is presented in the following sections.

2.2. Asymptotic scattering kernel

The scattering kernel of the resonance material can also be approximated by the asymptotic kernel

$$K_f(E' \to E) = \begin{cases} \dfrac{1}{(1-\alpha_f)E'} & \text{for } \alpha_f E' \le E \le E' \\ 0 & \text{otherwise} \end{cases}. \quad (5)$$

An implementation of this kernel in MCSD code is as follows. Consider a collision between a neutron of speed v' and a nucleus at rest in the laboratory system (LS). The underlying assumptions for the asymptotic kernel are 1) the nucleus is initially at rest in the LS and 2) the scattering is isotropic in the center-of-mass system (CMS). From energy conservation and momentum conservation principles, the following relation can be derived easily:

$$\frac{E}{E'} = \frac{A^2 + 2A\mu + 1}{(A+1)^2}, \quad (6)$$

where E' is the neutron energy before the collision in the LS, E is the neutron energy after the collision in the LS, μ is the direction cosine of the scattered neutron, relative to $\mathbf{v}'$ in the CMS, $\mathbf{v}'$ is the neutron velocity before the collision in the LS. Eq. (6) is used in the MCSD code for the asymptotic kernel with sampling of the angle, μ, based on isotropic scattering.

2.3. Exact scattering kernel

The exact scattering kernel can be written as

$$K_f(\mathbf{v}' \to \mathbf{v}) = \frac{1}{v'\sigma_s^{eff}(v')} \int\int v_r \sigma_s(v_r)\, p(\mathbf{v}' \to \mathbf{v}) M(\mathbf{V})\, d\mu\, d\mathbf{V}\,, \quad (7)$$

where $\sigma_s(v_r)$ is the scattering cross section at 0K, $\sigma_s^{eff}(v')$ is the Doppler-broadened cross section, $M(\mathbf{V})$ is the Maxwellian distribution, and $p(\mathbf{v}' \to \mathbf{v})$ is the probability that the scattered neutron with initial velocity $\mathbf{v}'$ will have final velocity $\mathbf{v}$. The direct numerical evaluation of p and the double integration is complicated, therefore a Monte Carlo method has been chosen to solve this neutron slowing down problem.

Consider a collision between a neutron of speed v' and a nucleus of speed V in the LS. The relationships for the conservation of energy and momentum lead to an expression for the velocity of an elastically scattered neutron which can be written as (Bell and Glasstone, 1968)

$$v = \sqrt{V_c^2 + \left(\frac{A}{A+1} v_r\right)^2 + 2V_c \left(\frac{A}{A+1} v_r\right)\mu}\,, \quad (8)$$

where

$$\mathbf{V}_c = \frac{\mathbf{v}' + A\mathbf{V}}{1+A} \text{ and } v_r = \sqrt{V^2 + v'^2 - 2v'V\mu'}\,,$$

and $\mathbf{v}'$ and E' are the neutron velocity and energy before the collision in the LS, $\mathbf{v}$ and E are the neutron velocity and energy after the collision in the LS, μ is the direction cosine of the scattered neutron, relative to $\mathbf{V_c}$ in the CMS, μ' is the direction cosine of the nucleus before collision, relative to $\mathbf{v}'$ in the LS, $\mathbf{V}$ is the velocity of the target in the LS, $\mathbf{V_c}$ is the velocity of the center of mass in the LS, and $\mathbf{v_r}$ is the velocity of the neutron relative to the target in the LS. Eq. (8) is used with the appropriate sampling of the angles μ and μ', and velocity of target, V. With the assumption that scattering is isotropic in the CMS, the direction cosine of outgoing neutron, μ, is sampled from a uniform pdf in the range [-1, +1].

2.4. The MCSD code

A simple infinite medium neutron slowing down code, named MCSD, was written to solve Eq. (3) with either the asymptotic or the exact scattering kernel.

2.4.1 Source neutron sampling

MCSD assumes a 1/E distribution of source neutrons over a user-specified energy range and then solves the neutron slowing down problem until neutrons are either absorbed or scattered to an energy below the resolved resonance region.

2.4.2 Cross section data

The MCSD code uses ENDF/B-VII.0 cross section data processed via NJOY to generate point-wise PENDF data of ^{238}U at 11 temperatures. MCSD linearly interpolates in the point-wise cross sections to evaluate cross sections at the requested neutron energies.

2.4.3 Tallies

Three major types of tallies are performed in MCSD. First is simply an edit for verification purposes, in which the scattering kernel, K_i (the probability that an incident neutron is scattered into the energy bin $[E_{i-1}, E_i]$), is tallied by

$$K_i(E' \to [E_{i-1}, E_i]) = T_i / N\,, \quad (9)$$

where N is the total number of incident neutrons and

$$T_i = \sum_{E_j \in [E_{i-1}, E_i]} w_j\,.$$

Second is the group-wise scalar flux, tallied as

$$\phi_g = \sum_{E_j \in g} d\, w_j\,, \quad (10)$$

where $d = -\frac{\ln(1-r)}{\sigma_t}$ and r is a random number.

Third is group-wise reaction rate for interaction type alpha, tallied as

$$R_{\alpha g} = \sum_{E_j \in g} \sigma_\alpha\, d\, w_j\,. \quad (11)$$

Using these tallied quantities, group absorption cross section is calculated by

$$\sigma_{ag} = \frac{R_{ag}}{\phi_g}\,, \quad (12)$$

and the absorption resonance integral is computed as

$$I_{ag} = \frac{\sigma_b}{\sigma_{ag} + \sigma_b} \sigma_{ag}\,, \qquad (13)$$

where σ_b is the user-defined background cross section which excludes the potential cross section of resonance isotope itself. The standard deviation of mean resonance integral, $\bar{I}$, is calculated by

$$\sigma_{\bar{I}} = \sqrt{\frac{\overline{I^2} - \bar{I}^2}{M(M-1)}}\,, \qquad (14)$$

where *M* is the number of batches,

$$\bar{I} = \frac{1}{M}\sum_m I_m \quad \text{and} \quad \overline{I^2} = \frac{1}{M}\sum_m I_m^2\,,$$

and I_m is the resonance integral of batch *m*.

2.4.4 Analog exact scattering kernel

One implementation of the exact scattering kernel in MCSD is the analog exact scattering kernel (AESK). In the AESK, the pdf for the velocity of the target nucleus, *V*, and the cosine angle of the collision between a neutron and a nucleus, μ', can be written as (Ouisloumen and Sanchez, 1991)

$$p(\mu', V) = v_r \sigma(\mu', V) M(V)\,, \qquad (15)$$

where

$$M(V) = 4\pi\left(\frac{m}{2\pi kT}\right)^{3/2} V^2 e^{-\frac{mV^2}{2kT}} \qquad (16)$$

is the Maxwellian distribution and *T* is the equilibrium temperature, *k* is the Boltzmann constant, and *m* is the mass of the target nucleus. This pdf has two independent variables, μ' and *V*. The cross section, σ, is a function of these two variables such that they cannot be sampled independently. Therefore, one can choose to sample angle first, based on the following pdf

$$p(\mu') = \tilde{\sigma}(\mu')\,, \qquad (17)$$

where

$$\tilde{\sigma}(\mu') = \int_0^\infty v_r \sigma(\mu', V) M(V)\, dV\,. \qquad (18)$$

The pdf for the speed of the nucleus becomes

$$p(V) = v_r(\mu_0')\,\sigma(\mu_0', V) M(V)\,, \qquad (19)$$

where μ_0' is assumed to be known, i.e., already sampled by Eq. (17).

2.4.5 Fast effective scattering kernel

The AESK kernel in the previous section is computationally inefficient because the right hand side of Eq. (18) has to be numerically integrated in every collision sampling during the neutron slowing down process. In order to improve the computational efficiency of the MC simulation, an accelerated non-analog version has been developed which will be called here as FESK – fast effective scattering kernel. In FESK, the two independent variables are sampled separately using their own pdfs and the weight of the neutron is updated appropriately. The pdf for the angle between the target nucleus and incident neutron is assumed to be uniform (isotropic), and the pdf for the speed of nucleus is the Maxwell-Boltzmann distribution *M(V)*. The weight of neutron is updated by

$$w = w \times \frac{\sigma_t(v_r)\frac{v_r}{v'} + \sigma_b}{\sigma_t^{eff}(v')\frac{v_r}{v'} + \sigma_b}\,, \qquad (20)$$

where σ_t is the total cross section at 0K, σ_t^{eff} is the Doppler-broadened total cross section to the temperature *T*, and σ_b is the background cross section. The Doppler-broadened cross sections are defined by

$$\sigma_\alpha^{eff}(v') = \frac{1}{v'}\int v_r \sigma_\alpha(v_r) M(\mathbf{V})\, d\mathbf{V}\,, \qquad (21)$$

where α is the type of reaction.

2.5. Resonance scattering kernel tests

The first tests for MCSD were to verify the implementation of the asymptotic and exact scattering kernels. For this purpose, neutrons were started at various energies and the resulting scattering kernels were tallied and compared with kernels published by Ouisloumen and Sanchez (1991). For neutron energies just below the peaks of the major ^{238}U absorption resonances (incident neutron energy 36.25 eV), the

exact kernels are quite different from the traditionally-assumed asymptotic kernels, as displayed in Fig. 1. Note that a larger fraction of scattered neutrons gain energy in a high temperature (1000K) material than in a low temperature (300K) material. Upscatter fractions computed with MCSD are compared to those of Ouisloumen and Sanchez (1991) in Table 1, and it can be seen that there is very close agreement, which one can interpret as a verification of the implementation of the exact scattering kernel in MCSD.

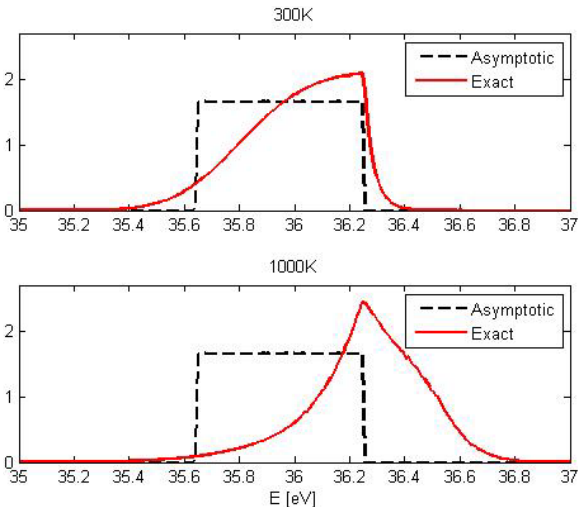

Fig. 1. ^{238}U scattering kernels at 36.25 eV

Table 1
Upscatter percentage at 1000K

Resonance (eV)	Neutron energy (eV)	O&S[1)]	FESK
6.67	6.52	82.03	83.40(0.042)[2)]
	7.20	28.12	28.20 (0.007)
36.67	36.25	54.23	55.28 (0.056)
	37.20	7.95	7.26 (0.011)
661.14	659.00	1.42	1.18 (0.034)
	664.00	0.84	0.74 (0.002)

1) Ouisloumen and Sanchez (1991)
2) One Sigma Standard Deviation

2.6. Variance reduction techniques

Use of the exact scattering kernels rather than traditional asymptotic kernels makes the solution of the neutron slowing down problem much more difficult to statistically converge. This is expected since the Monte Carlo simulation of the exact kernels samples for the target nucleus velocity and angle relative to the incident neutron, and the neutron cross sections in the vicinity of a resonance are extremely sensitive to the relative velocity. Consequently, it is extremely important to take advantage of numerous variance reduction techniques to improve simulation statistics.

The performance of numerous variance reduction techniques have been examined by solving the neutron slowing down problem over the neutron energy range of 53.6 ~ 27.2 eV for ^{238}U at 1000K and a background cross section of 60 barns and tallying resonance integrals from 47.9 to 27.7 eV (36.67 eV resonance).

The details of acceleration techniques will be described in the following sections. Table 2 summarizes a calculation with all accelerations and without acceleration. Each simulation employed 10 batches of 1 million source neutrons. The accelerations reduce variance by a factor of 12 for the asymptotic kernel and a factor of 7 for FESK kernel. The case with all accelerations takes a factor of two longer calculational time. So the computational efficiency is a factor of 25 improved with accelerations. The individual effects of each acceleration technique have been investigated and they are detailed in the following sections.

Table 2
Impact of all acceleration techniques

Acceleration	Resonance Integral (1 sigma)	
	Asymptotic	FESK
All	5.047 (0.0006)	5.284 (0.0026)
None	5.051 (0.0074)	5.283 (0.0191)

2.6.1 Exact slowing down vs. 1/E

One approximation that is often made when generating resonance integrals is that the source of neutrons is assumed to be 1/E in the resonance range. If this assumption is valid, the slowing down problem could be solved without need for the random component of source neutron energies that naturally result from the simulation process. To test this assumption, two simulations were performed: 1) source neutrons started from above 1000 eV and explicit slowing down (in hydrogen scatterer) past the

range of interest, and 2) source neutrons started from a uniform 1/E source over the energy range of interest. Results of these two simulations are summarized in Table 3.

Table 3
Impact of source neutron sampling

Sources	Resonance Integral (1 sigma)	
	Asymptotic	FESK
1/E	5.047 (0.0006)	5.284 (0.0026)
Exact	5.038 (0.0023)	5.284 (0.0080)

These results demonstrate that the 1/E approximation introduces only a very small bias (~0.2%) on the resonance integral relative to the difference between the asymptotic and exact scattering model (~ 4%) that is being studied. It is also clear from the relative statistics that starting neutrons in the 1/E spectra reduces the statistical variation of the resonance integral by a factor of roughly four. The 1/E assumption also reduces execution time in half by eliminating the MC slowing down simulation over the energy region from 1000 eV to the energy range of interest. Consequently, all subsequent simulations reported here use the 1/E source assumption to significantly improve statistics.

2.6.2 Uniform 1/E sources

When source neutrons are assumed to be 1/E, the cumulative distribution function (cdf) for the source neutron energy is

$$P(E) = \frac{\ln(E) - \ln(E_{\min})}{\ln(E_{\max}) - \ln(E_{\min})}, \qquad (22)$$

where $E_{\max}$ and $E_{\min}$ are the maximum and minimum energy of simulated source neutrons. Consequently, source neutrons can be sampled as

$$E = e^{\ln(E_{\min}) + r \cdot \ln(E_{\max}/E_{\min})}, \qquad (23)$$

where r is a random number between 0 and 1. However, since the source is assumed to be 1/E and since one starts a fixed number of neutrons per batch, there is no need to randomly place them in energy. Instead, one can simply use the 1/E cdf to uniformly distribute the source neutrons. This avoids variations that result from sampling source neutron energies. Table 4 presents a comparison of two simulations, one with uniform 1/E source neutron energies and one with random sampling of neutron energies. From Table 4 it is clear that forcing a uniform distribution of source neutrons reduces the statistical variation in resonance integral by a factor of approximately two. Consequently, all subsequent simulations reported here use the forced uniform source distribution to significantly improve the statistics of reported results.

Table 4
Impact of uniform source

Sources	Resonance Integral (1 sigma)	
	Asymptotic	FESK
Uniform	5.047 (0.0006)	5.284 (0.0026)
Random	5.045 (0.0053)	5.281 (0.0059)

2.6.3 Forced scattering interactions

In the computation of resonance integral, each collision with the background scatterer is assumed to scatter the neutron past the resonance range. Consequently, many neutrons are removed from simulation by interaction with the background scatterer, and it is extremely inefficient to simply start another source neutron. Instead, it is advantageous to force scattering interactions with the resonant scatterer at each collision. A comparison of resonance integrals with analog and forced scattering is presented in Table 5.

Table 5
Impact of forced scattering

Collisions	Resonance Integral (1 sigma)	
	Asymptotic	FESK
Forced	5.047 (0.0006)	5.284 (0.0026)
Random	5.040 (0.0075)	5.272 (0.0058)

These results demonstrate that at least a factor of two reduction of uncertainty is achieved by forcing scattering interactions. Since neutrons live longer when forced scattering is applied, execution times increase by a factor of three, but computational efficiency is still improved.

2.6.4 Sampling of distance to collision

In the homogeneous infinite medium studied here, the next collision is always in the same medium. Consequently, the distance to collision is only needed for track length estimates of fluxes and reaction rates. Since the distance to the next collision can be sampled with the cdf

$$P(d) = \int_0^d p(x)dx = 1 - e^{-\sigma_t d}, \qquad (24)$$

the distance to next collision is sampled from

$$d = -\frac{\ln(1-r)}{\sigma_t}. \qquad (25)$$

Rather than sampling for *d*, the expectation value $1/\sigma_t$ can be used directly for tallies. Results presented in Table 6 demonstrate that a factor of at least six reduction in uncertainty is obtained by using expectation values for the track length tallies of resonance integral.

Table 6
Impact of collision distance sampling

Distance	Resonance Integral (1 sigma)	
	Asymptotic	FESK
Expected	5.047 (0.0006)	5.284 (0.0026)
Random	5.040 (0.0087)	5.276 (0.0128)

2.6.5 Neutron splitting and Russian roulette

Traditional neutron splitting and Russian roulette are both effective means to reduce uncertainties. Table 7 presents a comparison of resonance integrals when the neutron splitting and Russian roulette are not used.

Table 7
Impact of neutron splitting and Russian roulette

	Resonance Integral (1 sigma)	
	Asymptotic	FESK
Splitting and RR	5.047 (0.0006)	5.284 (0.0026)
No RR	5.046 (0.0005)	5.279 (0.0027)
No Splitting	5.045 (0.0007)	5.285 (0.0103)

Splitting is extremely effective in improving statistics and Russian roulette is effective in reducing execution times (a factor of two), and both are employed in all subsequent simulations.

2.6.6 Simulation statistics

A sensitivity study of the resonance integral statistics (with all accelerations employed) to the number of neutron histories and number of batches is summarized in Table 8. The uncertainty of resonance integral has the expected variation with number of histories per batch and number of batches.

Table 8
Sensitivity to neutron histories

History (*1e+6)	Batch	Resonance Integral (1 sigma)	
		Asymptotic	FESK
1	10	5.047 (0.00065)	5.284 (0.00258)
1	40	5.046 (0.00048)	5.283 (0.00124)
1	160	5.046 (0.00025)	5.283 (0.00062)
1	640	5.046 (0.00012)	5.283 (0.00033)
4	10	5.046 (0.00030)	5.284 (0.00131)
16	10	5.046 (0.00019)	5.283 (0.00039)

2.6.7 AESK vs. FESK

Spectra for both an AESK and FESK simulation are observed to be nearly the same, as expected (FESK spectrum is displayed in Fig. 2). The AESK simulation has a resonance integral uncertainty that is roughly a factor of three smaller than the equivalent FESK simulation. The execution time of AESK simulation is 18,700 seconds, which is 470 times longer than the FESK simulation. Consequently, the overall performance of FESK is approximates 50 times more efficient than AESK, and is used here for all subsequent studies.

3. Neutron upscatter in scattering resonances

NJOY and MCSD calculated spectra near the ^{238}U 36.67 eV resonance are depicted in Fig. 2 for a 60 barn background scatterer. The NJOY spectrum clearly matches the MCSD spectrum computed with the asymptotic kernel. The FESK spectrum shows noticeable flux reductions near the flux peak at 35.8 eV and a slight shift to higher energies (the region of higher ^{238}U capture cross section), which results in an increase in absorption resonance integrals. Note that the resonance integrals displayed in Table 8 for the FESK are ~ 4% larger than that of asymptotic kernel.

4. Resonance upscatter correction for CASMO-5

CASMO-5 uses Bondarenko self-shielding tables to interpolate resonance integral for given temperature, *T*, and background cross section, σ_b. Note that these resonance integrals are normally generated directly from NJOY and do not account for the

resonance scattering effects discussed in this paper. The ^{238}U resonance upscatter effects are incorporated directly into CASMO-5 by using MCSD generated data rather than the NJOY data. CASMO-5 resonance integral tables have been generated for 18 background cross sections and 10 temperatures with 640M neutron histories (64M/batch * 10 batches) for each case.

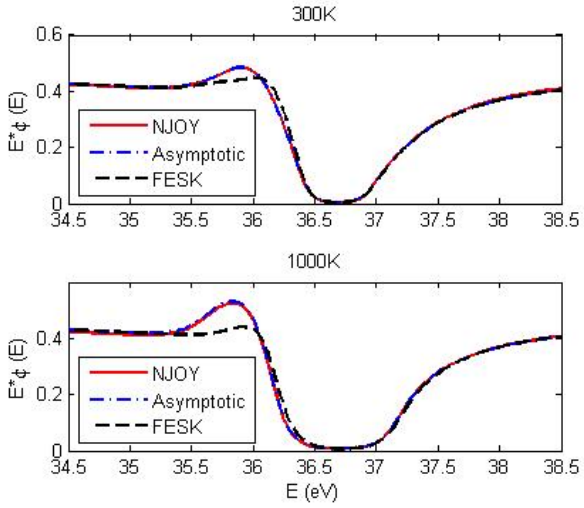

Fig. 2. Neutron spectrum at ^{238}U 36.68 eV resonance

5. CASMO-5 LWR Doppler coefficients

5.1. Doppler Pin-cell Benchmark

The UO_2 pin-cell Doppler benchmark of Mosteller (Mosteller, 2006, 2007) has been analyzed with CASMO-5 and ENDF/B-VII.0 (Oblozinsky and Herman, 2006). Doppler coefficients were calculated from eigenvalues at 600K (HZP) and 900K (HFP), and results are summarized in Fig. 3 and Table 9. MCNP5 results in Fig. 3 are taken from Mosteller (2006) who also used ENDF/B-VII.0 data. It can be observed from these results that the upscatter correction makes fuel temperature coefficients (FTC) more negative by 9 - 10%.

In examining the differences between MCNP5 and CASMO-5, MCSD was also modified to use the same elastic scattering assumptions of MCNP5. That is, Eq. (2) was used directly in the FESK kernel to generate data for CASMO-5. Doppler coefficients computed with this model have been observed to be even less negative than those without upscattering (e.g., -2.18 pcm/K at 4.5 w/o vs. -2.21 pcm/K of asymptotic kernel), and they are in closer agreement with the MCNP5 FTCs. By implication, the MCNP5 scattering model produces FTCs even more discrepant, relative to the exact scattering kernel, than the simple asymptotic model.

The impact of accurate modeling of resonance scattering grows rapidly with fuel temperature. For instance, in the 4.5 w/o enriched PWR lattice, the FESK model produces eigenvalues that are lower than the asymptotic model by 110 and 211 pcm at 600K and 900K, respectively. At 300K, the difference is only 32 pcm. This is extremely fortunate, as many MCNP5 cold criticals calculations have been used in the validation of ENDF/B-VII.0 data (Oblozinsky and Herman, 2006).

Table 9
Fuel temperature coefficients

Enrichment (w/o)	Asymptotic Kernel			FESK Kernel			FTC Diff (%)
	HZP	HFP	FTC[1)]	HZP	HFP	FTC	
0.711	0.66510	0.65891	-4.71	0.66451	0.65777	-5.13	-9.0
1.6	0.96076	0.95206	-3.17	0.95989	0.95039	-3.47	-9.5
2.4	1.09921	1.08950	-2.70	1.09821	1.08761	-2.96	-9.6
3.1	1.17732	1.16713	-2.47	1.17627	1.16512	-2.71	-9.7
3.9	1.24008	1.22955	-2.30	1.23900	1.22747	-2.53	-9.7
4.5	1.27556	1.26484	-2.21	1.27446	1.26273	-2.43	-9.7
5.0	1.29990	1.28908	-2.15	1.29878	1.28696	-2.36	-9.7

1) FTC = $(1/k_{hzp} - 1/k_{hfp})$ *1E+5 / 300 (pcm/K)

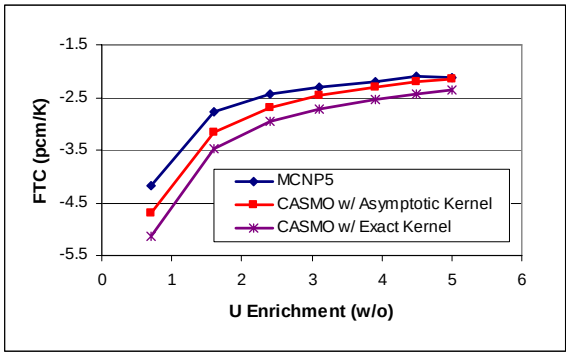

Fig. 3. Fuel temperature coefficients of UO_2 pin

5.2. *Resonance Scattering in NGNP Fuel*

To evaluate the impact of ^{238}U resonance scattering on NGNP fuel, a simple infinite medium of TRISO particles was examined. Typical design parameters of high temperature reactor (HTR) pebble fuel are shown in Tables 10 and 11, where the fuel kernel coating layers have been simplified to a single layer of SiC. Table 11 presents a simple transformation of the pebble sphere containing 1200 sphere fuel kernels to a cylinder pin-cell problem that can be computed by CASMO-5. The radius of cylinder fuel has been chosen to preserve the mean chord length of spherical fuel kernel. The thickness of the cylinder clad was computed to preserve the volume ratio of coating layer to fuel kernel. Pin pitch has been adjusted to preserve the fuel to moderator (coating layer + graphite matrix) volume.

Table 12 presents results for both LWR and HTR fuels computed with exact scattering kernel and the asymptotic scattering kernel. At typical HFP conditions, the exact scattering kernel effects in a PWR and an HTR are ~200 pcm and ~450 pcm, respectively. The effect of exact scattering kernel is insensitive to uranium enrichment in both reactors, but very sensitive to fuel temperature.

Table 10
HTR material specifications

Number of Kernels/Pebble	12000
Kernel Fuel	UO_2
UO_2 Density [g/cc]	10.36
Coating Material	SiC @ 1000K
Coating Density [g/cc]	3.4
Moderator Material	Graphite@1000K
Graphite Density [g/cc]	1.6

Table 11
HTR dimensions: sphere vs. cylinder model

	Spherical Model		Cylindrical Model	
Radius [cm]	Kernel	0.025	Fuel Pin	0.01667
Thickness [cm]	Coating	0.02	Clad	0.02358
Radius [cm]	Pebble	2.5	Pin Cell	0.26960
Fuel/Mod Ratio	Pebble	0.01215	Pin	0.01215

Table 12
Reactivity effect of exact scattering kernel

Fuel Temp (K)	Enrichment (w/o)	PWR			HTR		
		Asymptotic	FESK	Diff. (pcm)	Asymptotic	FESK	Diff. (pcm)
300	4	1.25994	1.25963	-31	1.21814	1.21821	8
	8	1.40550	1.40519	-30	1.33661	1.33671	10
	12	1.46695	1.46668	-28	1.38310	1.38321	11
900	4	1.23609	1.23401	-209	1.13643	1.13360	-283
	8	1.38006	1.37794	-212	1.25201	1.24914	-286
	12	1.44122	1.43921	-201	1.30066	1.29795	-271
1350	4	1.22298	1.21947	-352	1.09730	1.09287	-443
	8	1.36643	1.36284	-358	1.21182	1.20732	-450
	12	1.42775	1.42434	-340	1.26186	1.25758	-428

The ^{238}U exact scattering kernel has its biggest impact in the groups containing the 36.67 eV and 20.87 eV resonances, with 5% and 2% absorption increases, respectively. Since the ^{238}U absorption reaction in the HTR fuel is approximately 50% larger than in the PWR fuel, reactivity effects are proportionally larger.

6. Conclusions

The asymptotic elastic scattering models used in the epithermal energy range in NJOY and Monte Carlo codes lead to ~10% under prediction of Doppler coefficients of LWR lattices. Reactivity effects from implementing the exact scattering kernel are ~200 pcm for PWRs and ~450 pcm for NGNPs at HFP. Results presented here (computed via a totally independent computational approach) confirm the observations of numerous other researchers (Ouisloumen and Sanchez, 1991; Bouland et al.; Kolesov and Ukraintsev, 2006; Dagan and Broeders, 2006).

Consequently, until such time as the NJOY resonance elastic scattering model is improved, NJOY data used in downstream deterministic codes will introduce large systematic errors in thermal reactor eigenvalues and Doppler coefficients. The simple model presented here for implementation of resonance elastic scattering effects in CASMO-5 provides one example for circumventing current NJOY limitations. However, direct improvement in NJOY modeling of resonance elastic scattering is a preferable long- term path.

Likewise, Monte Carlo codes that make the asymptotic scattering approximation for heavy nuclide resonance scattering, like MCNP5, MCNP4C, MCNPX, O5R, SAM-CE, VIM, RCP, MVP, and TART, all currently suffer similar shortcomings (Brown, 2008). Until such time as these approximations are improved, caution should be used when considering Monte Carlo calculations as reference solutions for low-enriched uranium thermal-spectrum reactors.

It is straightforward to implement the methods presented here for sampling of target velocity and target nucleus/incident neutron scattering angle into any Monte Carlo code. However, obtaining statistically meaningful results will be far more difficult with sampling of the exact scattering kernels, and the required neutron histories may make most thermal reactor applications impractical. It should be noted that many of the acceleration methods discussed here are not directly applicable to general Monte Carlo applications, and additional work in the Monte Carlo community will be required to efficiently address the resonance scattering issues detailed here.

References

Bell, G. I., Glasstone, S., 1968. Nuclear Reactor Theory. Robert E. Krieder Publishing Co.

Bouland, O., Kolesov, V., Rowlands, J.L., The Effect of Approximations in the Energy Distributions of Scattered Neutrons on Thermal Reactor Doppler Effects. JEF/DOC-486.

Brown, F., 2008. Personal Communication.

Carter, L.L., Cashwell, E.D., 1975. Particle-Transport Simulation with the Monte Carlo Method. Los Alamos Scientific Laboratory.

Dagan, R., Broeders, C.H.M., 2006. On the Effect of Resonance Dependent Scattering-kernel on Fuel Cycle and Inventory. PHYSOR-2006, Vancouver, Canada.

Kolesov, V.V., Ukraintsev, V.F., 2006. Temperature Effects and Resonance Elastic Cross Section Influence on Secondary Energy Distributions of Scattered Neutrons in the Resolved Resonance Region. PHYSOR-2006, Vancouver, Canada.

MacFarlane, R.E., Muir, D.W., 2000. NJOY99.0 Code System for Producing Pointwise and Multigroup Neutron and Photon Cross Sections from ENDF/B Data. PSR-480/NJOY99.00, Los Alamos National Laboratory, Los Alamos.

Mosteller, R.D., 2006. Computational Benchmark for the Doppler Reactivity Defect. LA-UR-06-2968, Los Alamos National Laboratory.

Mosteller, R.D., 2007. ENDF/B-V, ENDF/B-VI, and ENDF/B-VII.0 Results for the Doppler-defect Benchmark. M&C+SNA 2007, Monterey, CA.

Oblozinsky, P., Herman, M., 2006. Special Issue on Evaluated Nuclear Data File ENDF/B-VII.0. Nuclear Data Sheets, Volume 107, Number 12.

Ouisloumen, M., Sanchez, R., 1991. A Model for Neutron Scattering off Heavy Isotopes that Accounts for Thermal Agitation Effects. Nucl. Sci. Eng., 107, pp. 189-200.

Rhodes, J., Smith, K., Lee, D., 2006. CASMO-5 Development and Applications. PHYSOR-2006, Vancouver, Canada.

X-5 Monte Carlo Team, 2003. MCNP – A General Monte Carlo N-Particle Transport Code, Version 5. LA-CP03-0245.